A minute Meckel’s cartilage from the Devonian Hangenberg black shale in Morocco and its position in chondrichthyan jaw morphospace (#76196)

First submission

Guidance from your Editor

Please submit by **26 Aug 2022** for the benefit of the authors (and your $200 publishing discount) .

Structure and Criteria
Please read the 'Structure and Criteria' page for general guidance.

Custom checks
Make sure you include the custom checks shown below, in your review.

Raw data check
Review the raw data.

Image check
Check that figures and images have not been inappropriately manipulated.

Privacy reminder: If uploading an annotated PDF, remove identifiable information to remain anonymous.

Files

Download and review all files from the materials page.

6 Figure file(s)
1 Table file(s)
1 Raw data file(s)

Custom checks

Field study

- Have you checked the authors field study permits?
- Are the field study permits appropriate?

Structure your review

The review form is divided into 5 sections. Please consider these when composing your review:

1. **BASIC REPORTING**
2. **EXPERIMENTAL DESIGN**
3. **VALIDITY OF THE FINDINGS**
4. General comments
5. Confidential notes to the editor

You can also annotate this PDF and upload it as part of your review

When ready submit online.

Editorial Criteria

Use these criteria points to structure your review. The full detailed editorial criteria is on your guidance page.

BASIC REPORTING

- Clear, unambiguous, professional English language used throughout.
- Intro & background to show context. Literature well referenced & relevant.
- Structure conforms to PeerJ standards, discipline norm, or improved for clarity.
- Figures are relevant, high quality, well labelled & described.
- Raw data supplied (see PeerJ policy).

EXPERIMENTAL DESIGN

- Original primary research within Scope of the journal.
- Research question well defined, relevant & meaningful. It is stated how the research fills an identified knowledge gap.
- Rigorous investigation performed to a high technical & ethical standard.
- Methods described with sufficient detail & information to replicate.

VALIDITY OF THE FINDINGS

- Impact and novelty not assessed. *Meaningful* replication encouraged where rationale & benefit to literature is clearly stated.
- All underlying data have been provided; they are robust, statistically sound, & controlled.
- Conclusions are well stated, linked to original research question & limited to supporting results.

Standout reviewing tips

The best reviewers use these techniques

Tip	*Example*
Support criticisms with evidence from the text or from other sources	*Smith et al (J of Methodology, 2005, V3, pp 123) have shown that the analysis you use in Lines 241-250 is not the most appropriate for this situation. Please explain why you used this method.*
Give specific suggestions on how to improve the manuscript	*Your introduction needs more detail. I suggest that you improve the description at lines 57- 86 to provide more justification for your study (specifically, you should expand upon the knowledge gap being filled).*
Comment on language and grammar issues	*The English language should be improved to ensure that an international audience can clearly understand your text. Some examples where the language could be improved include lines 23, 77, 121, 128 – the current phrasing makes comprehension difficult. I suggest you have a colleague who is proficient in English and familiar with the subject matter review your manuscript, or contact a professional editing service.*
Organize by importance of the issues, and number your points	*1. Your most important issue* *2. The next most important item* *3. …* *4. The least important points*
Please provide constructive criticism, and avoid personal opinions	*I thank you for providing the raw data, however your supplemental files need more descriptive metadata identifiers to be useful to future readers. Although your results are compelling, the data analysis should be improved in the following ways: AA, BB, CC*
Comment on strengths (as well as weaknesses) of the manuscript	*I commend the authors for their extensive data set, compiled over many years of detailed fieldwork. In addition, the manuscript is clearly written in professional, unambiguous language. If there is a weakness, it is in the statistical analysis (as I have noted above) which should be improved upon before Acceptance.*

A minute Meckel's cartilage from the Devonian Hangenberg black shale in Morocco and its position in chondrichthyan jaw morphospace

Merle Greif [Corresp., 1], **Humberto Ferrón** [2], **Christian Klug** [1]

[1] Palaeontological Institute and Museum, University of Zürich, Zürich, Switzerland

[2] Instituto Cavanilles de Biodiversidad i Biología Evolutiva, Universitat de València, 46980 Paterna, Valencia,, Spain

Corresponding Author: Merle Greif
Email address: merle.greif@pim.uzh.ch

Chondrichthyan remains are mostly known from their teeth or fin spines only, whereas their cartilaginous endoskeletons require exceptional preservational conditions to become fossilized. While most cartilaginous remains of Famennian chondrichthyans were found in older layers of the eastern Anti-Atlas, such fossils were unknown from the Hangenberg black shale (HBS) and only a few chondrichthyan teeth had been found therein previously. Here, we describe a Meckel's cartilage from the Hangenberg black shale in Morocco, which is the first fossil cartilage from these strata. Since no teeth or other skeletal elements have been found in articulation, we used elliptical Fourier (EFA), principal component (PCA), and hierarchical cluster (HCA) analyses to morphologically compare it with 41 other chondrichthyan taxa and to evaluate its possible affiliation. Additionally, a mantel test was performed to evaluate the relationship between jaw shape and phylogenetic distances. PCA and HCA position the new specimen closest to some acanthodian and elasmobranch jaws. Accordingly, a holocephalan origin was excluded. The jaw shape as well as the presence of a polygonal pattern, typical for tessellated calcified cartilage, suggest a ctenacanth origin and we assigned the new HBS Meckel's cartilage to the order Ctenacanthiformes with reservations.

A minute Meckel's cartilage from the Devonian Hangenberg black shale in Morocco and its position in chondrichthyan jaw morphospace

Merle Greif[1], Humberto G. Ferrón[2], Christian Klug[1]

[1] Palaeontological Institute and Museum, University Zurich, 8006, Zurich, Switzerland.
[2] Instituto Cavanilles de Biodiversidad i Biología Evolutiva, Universitat de València, C/ Catedrático José Beltrán Martínez, 2, 46980 Paterna, Valencia, Spain; humberto.ferron@bristol.ac.uk, School of Earth Sciences, University of Bristol, Life Sciences Building, Bristol BS8 1TH, UK.

Corresponding Author:
Merle Greif[1]
University Zurich, Karl-Schmid-Strasse 4, 8006, Zurich, Switzerland.
Email address: merle.greif@pim.uzh.ch

Abstract

Chondrichthyan remains are mostly known from their teeth or fin spines only, whereas their cartilaginous endoskeletons require exceptional preservational conditions to become fossilized. While most cartilaginous remains of Famennian chondrichthyans were found in older layers of the eastern Anti-Atlas, such fossils were unknown from the Hangenberg black shale (HBS) and only a few chondrichthyan teeth had been found therein previously. Here, we describe a Meckel's cartilage from the Hangenberg black shale in Morocco, which is the first fossil cartilage from these strata. Since no teeth or other skeletal elements have been found in articulation, we used elliptical Fourier (EFA), principal component (PCA), and hierarchical cluster (HCA) analyses to morphologically compare it with 41 other chondrichthyan taxa and to evaluate its possible affiliation. Additionally, a mantel test was performed to evaluate the relationship between jaw

shape and phylogenetic distances. PCA and HCA position the new specimen closest to some acanthodian and elasmobranch jaws. Accordingly, a holocephalan origin was excluded. The jaw shape as well as the presence of a polygonal pattern, typical for tessellated calcified cartilage, suggest a ctenacanth origin and we assigned the new HBS Meckel's cartilage to the order Ctenacanthiformes with reservations.

Introduction

The supposedly oldest gnathostomes (jawed vertebrates) date back to the Ordovician period but are well documented from the Silurian (Brazeau & Friedman 2015). While only the arguably paraphyletic placoderms (King et al. 2017) and osteichthyans (bony fishes and tetrapods) are known from the Silurian, fossil chondrichthyans (sharks, rays and chimaeroids) are known only from the Devonian onward (Brazeau & Friedmann 2015) while the earliest acanthodian finds date back to the Silurian (Burrow & Rudkin 2014). Because of their quite basal position in the vertebrate stem and the great morphological disparity of body outlines, fin spines as well as types of dentitions, the phylogenetic position of acanthodians was widely discussed during the past decades (Hanke & Wilson 2006; Brazeau 2009; Davis et al. 2012; Burrow & Rudkin 2014; Brazeau & Friedman 2015; Brazeau & Winter 2015; Giles et al 2015; Qiao et al. 2016). Members of this group show characteristics of both principal lineages of living gnathostomes, are covered with scales and are often referred to as "spiny sharks" because of the spines in front of their dorsal, anal and paired fins (Qiao et al. 2016). Recently, acanthodians were recognized as stem chondrichthyans (Zhu et al. 2013; Coates et al. 2017; Rücklin et al. 2021).

Only teeth and fin spines of chondrichthyans (whole group, including acanthodians) are strongly mineralized while chondrichthyan endoskeletons are made of unmineralized cartilage covered by a thin layer of calcified cartilage (Kemp & Westrin 1979; Dean & Summers 2006, Seidel et al. 2016, 2020; Maisey et al. 2020) that is only rarely preserved. This thin outer layer shows a distinct polygonal pattern caused by the presence of tesserae – the tessellated calcified cartilage (Seide et al. 2016, 2020, 2021; Maisey et al. 2020). Such cartilage is characteristic for modern, as well as Devonian crown chondrichthyans (elasmobranchs and holocephalans, Long et al. 2015; Maisey 2020) while these polygonal structures tend to be less distinct in acanthodians, where only “subtessellated calcified cartilage” or “globular calcified cartilage” is reported (Dean & Summers 2006; Brazeau & Friedman 2014; Maisey et al. 2020).

Among the cartilaginous remains, jaws are one of the most relevant anatomical structures from an evolutionary perspective. The evolution of lower jaws, the Meckel’s cartilage, is seen as a key innovation of gnathostomes enabling the first gnathostomes to broaden their range of feeding strategies and prey upon a much greater diversity of animals (DeLaurier & Gerhart, 2018; Deakin et al. 2022). These innovations contributed to their radiation and possibly to the decline of agnathans (Brazeau & Friedman 2015; Hill et al. 2018). Nevertheless, only very few quantitative studies about jaw shapes have been published. Hill et al. (2018) quantified jaw shape in modern and in Palaeozoic fishes and demonstrated that jaw shape has a greater disparity in modern fish clades than during the early gnathostome radiation (Silurian and Devonian). This is mostly caused by the great morphological disparity among modern actinopterygians (Hill et al. 2018). Deakin et al. (2022) also mentioned an increasing disparity in jaw shape with

ongoing evolution but the functional disparity of early vertebrate jaws to be highest very early in jaw evolution and optimized for a predatory function.

Despite chondrichthyan skeletons are frequently found in the middle and late Famennian strata in the Tafilalt and Maïder regions of southern Morocco (Ginter et al. 2002; Derycke et al. 2008; Frey et al. 2018; Frey et al. 2020), the Hangenberg black shale of Morocco constitutes an exception to this. The only vertebrate remains that are known from these strata are chondrichthyan teeth (Klug et al 2016; Frey et al. 2018). Additionally, some chondrichthyan ichnofossils were found in layers just above the Hangenberg black shale (basal Hangenberg Sandstone) (Klug et al 2021).

Here we describe a minute lower jaw found in the Anti-Atlas that represents the first reported cartilaginous remain from the Moroccan Hangenberg black shale, shedding light into the diversity of jaw morphologies seen in early gnathostomes. We have applied elliptical Fourier (EFA), principal component (PCA) and hierarchical cluster analyses (HCA) to the new small Meckel's cartilage and other chondrichthyan and acanthodian lower jaws, in order to approximate its possible systematic affiliation.

Geological setting – Hangenberg crisis

In the Anti-Atlas, sedimentary successions from the Late Proterozoic (Letsch et al. 2019) to the Early Carboniferous (Destombes & Hollard 1988) are well exposed. The Late Devonian Hangenberg crisis is a global extinction event at the Devonian-Carboniferous boundary (Caplan & Bustin 1999; Kaiser et al. 2011). It reflects one of the six largest mass extinction events in earth's history, and follows the Kellwasser

event at the Frasnian/Famennian boundary, which is categorized as one of the “Big Five” (McGhee 1996; McGhee et al 2012,2013).

The Hangenberg crisis affected vertebrate groups to an extent that is comparable to the Big Five mass extinctions. Therefore, it is seen as a bottleneck in vertebrate evolution and the recovery of formerly diverse vertebrate groups after the event was minimal (Sallan and Coates 2010; Frey et al. 2018). Indeed, the Hangenberg crisis was more severe than formerly thought and caused a larger diversity loss on genus level (32%) than the Kellwasser event (19%; Sallan & Coates 2010).

The Hangenberg crisis is recognizable by lithological changes such as the widespread appearance of black shales and sandstones in alternation all over the world (Kaiser et al. 2015; Becker et al. 2016; Paschall et al. 2019; Pisarzowska et al. 2020, Deng et al. 2021; DaSilvia et al. 2022). Short term climatic fluctuations, leading to changes in the carbon cycle, might have led to the differences in facies. Possible causes for these fluctuations are widely discussed and range from intense global transgressions (Sandberg et al. 1988; Chen et al. 2002, 2013), methylmercury poisoning due to volcanism (Racki et al. 2018; Rakociński et al. 2020; Pisarzowska et al. 2020), tectonic processes and associated tsunamis (Du et al. 2008), anoxia by various causes (Algeo & Scheckler 1998; Tribovillard et al. 2004), a supernova (Fields et al. 2020) to meteorite impacts (McGhee 1996; Morrow & Sandberg 2005). One of the most plausible hypothesis explaining some of the known macroecological changes is the global rise of land plants and particularly forests (Algeo & Scheckler 1998: p. 113)

The Hangenberg crisis is often divided into three stages. In the Rhenish massif, the first stage is characterized by sandstone layers (Drewer sandstone) and represents a drastic

sea-level fall and regression below the Hangenberg black shale that is connected to a short-lived glacial pulse in northern Gondwana at this time (Kaiser et al 2011, 2015). The Drewer sandstone is not developed in the eastern Anti-Atlas. This interval is followed by the Hangenberg black shale. In Morocco, the Hangenberg black shale was laid down during a supposed global transgression, which was linked with widespread anoxia, likely caused by eutrophication (Algeo & Scheckler 1998). In the Anti-Atlas, the black shale contains abundant algal remains, questioning the supposed transgressive character of these deposits. Widespread anoxia and the ceasing carbonate production led to global extinctions of numerous invertebrate and vertebrate groups at the early stage of the Hangenberg crisis with its culmination when the Hangenberg black shale formed (Sallan & Coates 2010; Kaiser et al 2011, 2015). The second stage is characterized by shales and sandstones, which were deposited during a subsequent regression interval (Kaiser et al. 2015). The third stage is characterized by the renewed growth of carbonate platforms in the early Tournaisian in many parts of the world. In Morocco, deposition of shales persisted until the middle Tournaisian (Kaiser et al. 2011, 2015). The Hangenberg black shale and sandstone crop out over vast areas in the eastern Anti-Atlas and give the opportunity to collect data to analyse processes that occurred around this crisis, its causes and its influence on biodiversity and particularly on early vertebrates.

Materials & Methods

The specimen PIMUZ A/I 5139 (Fig.1) was found during a field trip to the Moroccan Anti-Atlas at the locality Madene El Mrakib (N30.73093°, W4.70749°). Permit for fossil

collection and export were given by the Ministère de l'Energie, des Mines, de l'Eau et de l'Environnement, Rabat, Morocco. It is stored at the Palaeontological Institute and Museum of Zurich (Switzerland). The specimen was largely exposed, but covered parts were carefully prepared using a thin steel-needle. Photos were taken using a Nikon D2X and colour and contrast were adjusted in Adobe Photoshop (Adobe Inc. 2019). Close-ups were taken with a Leica MZ16 F microscope and adjusted in colour and contrast as well.

Morphometrics

Outlines of the lower jaws of 41 representatives of all important chondrichthyan (including acanthodians) orders were drawn using the vector-based software Affinity Designer based on photographs and illustrations from the literature (App. 1). These jaws belong to taxa from different periods and localities and cover a wide range of sizes. All Meckel's cartilage outlines were digitized in TPS software (Rohlf, 2015). Elliptic Fourier analysis (EFA) was then performed in the Momocs package (Bonhomme et al., 2014) in R (R Development Core Team, 2020) considering a total number of 25 harmonics, which gather nearly 99% of the cumulative harmonic power (considered as a measure of shape information) and reconstructs actual morphologies with high accuracy. We obtained a virtual morphospace by performing a principal component analysis (PCA, Fig. 2) on the preordination data. In order to quantify the morphological similarity amongst the studied jaws we performed a hierarchical cluster analysis (HCA) using the R package 'dendextend' (Galili et al. 2019). In order to assess the degree of morphological convergence in our sample, we performed a Mantel test correlating

phenetic (morphological) and phylogenetic distances. These metrics are expected to show greater decoupling and, consequently, lower correlation where homoplasy occurs. We repeated the test in a set of 1000 trees that accounted for phylogenetic and stratigraphic uncertainty. The tree topology is based on Klug et al. (in prep). Polytomies were randomly resolved 1000 times and each resulting tree was calibrated by randomizing the tip age of every species within the chronostratigraphic unit, at age or subperiod rank, where their first appearance occurs, using the R package ‘paleotree’.

Abbreviations

HBS: Hangenberg Black Shale; PCA: Principal Component Analysis; HCA Hierarchical Cluster Analysis, EFA: Elliptical Fourier Analysis

Results

Systematic Palaeontology

Class Chondrichthyes Huxley, 1880

Subclass ? Elasmobranchii Bonaparte, 1838

Order ? Ctenacanthiformes Glikman, 1964

The minute Meckel’s cartilage with a total length of 18 mm and a height of up to 6 mm is nearly complete (Fig. 1A). In the main fossil plate and in the counterpart, a distinctive polygonal pattern of the calcified cartilage is visible mainly in the posterior part (Fig. 1B). It shows a bright grey to white colour and is somewhat brighter than the sediment. The tessellation is not as geometric as in some modern species (Seidel et al. 2020,2021) but

a clear pattern is visible. The ventral edge of the Meckel's cartilage is gently convexly curved. The ventral ridge is discernible in spite of the compaction especially in the middle to posterior part. The Meckel's cartilage becomes higher from posteriorly until just before the articulation. It displays one bulge at the thickened anterior end, which is about 4 mm long and might represent the symphysis as well as the muscle attachment. This bulge is followed by a shallow depression, which is 3.5 mm long and a shallow bulge of about 2.5 mm length. We assume that the anterior 9 mm were the tooth-bearing part. The next depression extends over 7.5 mm and ends at the articulation. The posterior part is somewhat incomplete in the main plate and entirely missing in the counterpart (Fig. 1A, B). Although the specimen is flattened, the retroarticular flange (cf. Long et al. 2015) at the posterior end is still preserved as a knob.

Statistical Analyses

The PCA shows a good separation between the jaws of Elasmobranchii and Holocephalii (Fig. 2). PC 1 (59% of variance) is mostly related to changes in jaw thickness with decreasing thickness from negative to positive scores. PC 2 (13% of variance) mainly reflect changes of the jaw curvature (from strongly convex to slightly concave), with a decrease in curvature from negative to positive scores (Fig. 2). PC 3 (6% of variance) mostly depends on changes in the curvature of the anterior end of the jaws as well as changes of the roundness of the posteroventral edge of the jaws (Fig. 2). Holocephalan jaws occupy high PC1 scores of about 0.05 to 0.17 and positive PC2 scores and are restricted to the middle to upper right side of the morphospace. All holocephalan jaws show relatively slender and only slightly curved morphologies.

Elasmobranch jaws occupy a wider score range with PC1 scores between -0.8 to 0.08 and PC2 scores between 0.07 and 0.10 (Fig. 2). Most of them plot in the centre of the morphospace between PC1 scores of about -0.5 and 0.01 and PC2 scores around 0.0. Elasmobranch jaws show a greater shape variation, from thick and bulky to relatively slender. Acanthodian jaws occupy PC1 scores from -0.11 to 0.1 and PC2 scores of -0.12 to 0.05 (Fig. 2) and overlap to a large extent with elasmobranch and holocephalan jaws. Acanthodian jaw shapes vary from bulky and curved to slender and straight. The new specimen plots at -0.01/0.025 (PC1/PC2) close to other acanthodians and some elasmobranchs. The closest taxa are the acanthodians *Ischnacanthus sp. and Latviacanthus ventspilsensis.* Some Ctenacanths plot very close: *Dracopristis hoffmanorum, Ctenacanthus sp. Heslerodus divergens,* as well as another elasmobranch of the order Synechodontiformes*: Palidiplospinax occultidens* (Fig. 2). In the dendrogram derived from the HCA, the new Hangenberg black shale Meckel's cartilage plots closest to the acanthodian *Latviacanthus ventspilsensis*. The acanthodian *Ischnacanthus sp.* and the elasmobranch of *Heslerodus divergens* constitute sequential outgroups to those two (Fig. 3). Overall, a clear grouping regarding the three classes is not evident (Fig. 3) but at lower clustering rank, a separation between holocephalans and elasmobranchs is supported. Acanthodians often plot together with either elasmobranchs or holocephalans (Fig. 3). This pattern entails an important degree of homoplasy in the jaws of those groups, which is further supported by the absence of correlation in any of the 1000 performed Mantel tests (R statistic = -0.045 ± 0.009; *p*-value = 0.632 ± 0.032, data expressed in mean ± standard deviation).

Discussion

Both, the PCA and the HCA reveal that the outline morphology of the new Hangenberg black shale jaw is most similar to those seen in elasmobranchs and acanthodians. A holocephalan affinity is unlikely as all holocephalan jaws show distinctively different shapes (Fig. 2, 3). Whether the Hangenberg black shale jaw is of acanthodian or of elasmobranch origin is difficult to tell from the plots alone. In both plots, a slightly closer relation to acanthodian jaw shapes than to elasmobranch jaw shapes is apparent making an acanthodian affiliation likely (Fig. 2,3). The acanthodian jaws of *Ischnacanthus* and *Latviacanthus* are plotting closest to the new jaw. Two more Ctenacanth jaws plot close to the new HBS jaw, the ones of *Ctenacanthus sp*. and *Dracopristis hoffmanorum* and a little further away, the jaw of *Heslerodus divergens*. Regarding the PCA and HCA, either an acanthodian or an elasmobranch origin of the jaw is likely.

However, it has to be kept in mind, that PCA and HCA compare the two-dimensional outline shape of the 42 sampled lower jaws. Actually, the Mantel tests (Fig. 4) reveal the presence of an important homoplasy, which might hinder the interpretations of phylogenetic affinity from those analyses. Similarities in jaw shape can also result from adaptation. Jaw shape can, for example, be an adaption to a certain lifestyle as in durophagous sharks (Herbert & Motta 2018) or in general be connected to diet in combination with water depth (Motta & Huber 2012). Small variations in shape could also occur due to fossilisation, preparation and errors in redrawing the different outlines. Besides the HBS Meckel's cartilage, the only vertebrate fossils known from the Hangenberg black shale are some poorly preserved chondrichthyan teeth (Klug et al.

2016), which are not determined but could be of symmoriiform origin (? *Stethacanthus*, Coates & Sequeira 2001, fig. 5 F-I). Even though homoplasy is suggested we assume a holocephalan origin as unlikely since all holocephalan jaw shapes are entirely different and it is well conceivable that these teeth belonged to a different animal than the new HBS jaw.

The jaw of the ctenacanth *Heslerodus divergens* (Hodnett et al. 2021) seems to share some features not directly captured by outline analysis, that are less distinct in both acanthodian jaws that plot close to the HBS jaw. The jaw of *Heslerodus divergens* has a relatively thin anterior to middle part comparable to the first 9 mm of the new jaw that we described as the probable tooth bearing part. Following this, in both jaw shapes, a ridge is present leading to a second depression that ends in the articulation. In the jaw of *Heslerodus divergens* this shape is more distinct than in the HBS jaw while both acanthodian jaws are dorsally straighter shaped (Fig. 5). Additionally, Hodnett et al. (2021) describes "*a well-developed ventral ridge on the lateral margin of the Meckel's cartilage, that extends over two thirds the length of the jaw"*, as a synapomorphy of ctenacanths. A ventral ridge is one of the few features of the new Hangenberg black shale jaw, that is well recognizable (Fig. 1).

A complementary character that could help to determine the phylogenetic affinity of the HBS Meckel's cartilage is the structure of the cartilage. A distinct polygonal structure is visible on the surface of the jaw (Fig. 1C). This pattern is characteristic for tessellated calcified cartilage, which is now widely accepted as a synapomorphy of modern and extinct crown chondrichthyans (Brazeau & Friedman 2014; Long, et al. 2015; Seidel et al. 2016, 2021; Maisey et al. 2020), while osteichthyan fishes show a continuous

surface layer of perichondral bone (Brazeau et al. 2020; Maisey et al. 2020). In fossils of the acanthodian group, this polygonal structure is less distinct and not all species show this pattern (Maisey et al. 2020). However, in certain acanthodians like *Climatius* (Burrow et al. 2015)*, Ischnacanthus* (Burrow et al. 2018) or *Cheiracanthus* (den Blaauwen 2019*)*, similar structures are present. Maisey et al. (2020) described these as "*subtessellated perichondral biomineralization that could represent evolutionary precursors of tessellated calcified cartilage*" but real tessellated calcified cartilage is apparently absent in acanthodians (Brazeau & Friedman 2014). A polygonal pattern is evident but the borders of the single tesserae are a bit blurred taphonomically, which might have been caused by dissolution of collagen between the tiles. The presence of the pattern is a good evidence for a chondrichthyan total group affinity but the preservation of the new HBS jaw hinders a reliable assignment within the stem or crown group. However, since the polygonal pattern is distinct at the surface of the specimen, an elasmobranch origin appears more likely than an acanthodian origin. Acanthodians in general show a more granular surface and the sub-tessellated pattern shows up only in thin sections (Carole Burrow, personal communication, 23.07.2022). In *Ischnacanthus,* subtessellated calcified cartilage is present while it is not reported from *Latviacanthus.* An ischnacanth affiliation of the new Hangenberg black shale jaw, therefore, is possible (Fig. 6). The more likely origin seems to be an elasmobranch origin. With the jaw of *Heslerodus divergens* being the most similar elasmobranch shape, also sharing some other features, we assigned the new Meckel's cartilage to the order Ctenacanthiformes with reservations (Fig. 6).

To some degree, this classification remains provisional/tentative and a bigger sample size could help to test the hypothesis. Further fossil finds, as well as a better understanding of the early development of tessellated calcified cartilage in early fishes could also help to classify the new jaw in more detail.

Conclusions

The newly described Meckel's cartilage is the first known fossil cartilage remain from the Hangenberg black shale from the Moroccan Anti-Atlas. It is only 18 mm long, ventrally convexly curved and shows two depressions dorsally. PCA and HCA reveal a strong similarity in shape with some acanthodians and some elasmobranchs. The only other vertebrate fossils that are known from the same strata are of probable symmoriid origin and we assume that they are of a different affinity, as we excluded a holocephalan/ symmoriid origin based on the PCA and HCA. However, the Mantel test reveals an important homoplasy and phylogenetic interpretations of the analyses have to be seen with reservations. Furthermore, some similar features, that cannot be captured by outline analysis can be seen in the ctenacanth *Heslerodus divergens*, which shows a similarly curved dorsal edge and a distinct ventral ridge. These features are less distinct in the other acanthodian jaws that plot close. Additionally, the surface of the HBS Meckel's cartilage shows a distinct polygonal pattern that supports an elasmobranch origin rather than an acanthodian origin and we assigned the new lower jaw to the order Ctenacanthiformes, tentatively.

Acknowledgements

We thank the Ministère de l'Energie, des Mines, de l'Eau et de l'Environnement (Direction du Développement Minier, Division du Patrimoine, Rabat, Morocco) for providing working and sample export permits. At an earlier stage, Louis Dudit (Zürich) helped with the Fourier analysis. We showed photos of the Meckel's cartilage to Carole Burrow (Queensland) and Jake Leyhr (Uppsala) and discussed its affiliation. We greatly appreciate their suggestions regarding both the jaw and the teeth from the HBS. We thank the reviewers for XX.

References

Adobe Inc. 2019: *Adobe Photoshop*, Available at: https://www.adobe.com/products/photoshop.html

Algeo, T. J. and Scheckler, S. E. 1998: Terrestrial-marine teleconnections in the Devonian: links between the evolution of land plants, weathering processes, and marine anoxic events. *Philosophical Transactions of the Royal Society London* B353, 113–130.

Bapst, D. W. 2012: "paleotree: an R package for paleontological and phylogenetic analyses of evolution." *Methods in Ecology and Evolution* 3.5, 803-807.

Becker, R. T.; Kaiser, S. I.; Aretz, M. 2016: Review of chrono-, litho- and biostratigraphy across the global Hangenberg Crisis and Devonian–Carboniferous Boundary. Geological *Society, London, Special Publications,* 423, 355-386.

Bonhomme, V.; Picq, S.; Gaucherel, C.; Claude, J. 2014: Momocs: outline analysis using R. *Journal of Statistical Software* 56:1–24.

Brazeau, M. D. 2009: The braincase and jaws of a Devonian 'acanthodian' and modern gnathostome origins. *Nature* 457 (7227), 305–308.

Brazeau, M. D. 2012: A revision of the anatomy of the Early Devonian jawed vertebrate *Ptomacanthus anglicus* Miles. *Palaeontology* 55 (2), 355–367.

Brazeau, M. D.; Friedman, M. 2014: The characters of Palaeozoic jawed vertebrates. *Zoological Journal of the Linnean Society* 170 (4), 779–821.

Brazeau, M. D.; Giles, S.; Dearden, R. P.; Jerve, A.; Ariunchimeg, Y. A.; Zorig, E. et al. 2020: Endochondral bone in an Early Devonian 'placoderm' from Mongolia. *Nature Ecology and Evolution* 4 (11), 1477–1484.

Brazeau, M. D. & de Winter, V. 2015: The hyoid arch and braincase anatomy of *Acanthodes* support chondrichthyan affinity of 'acanthodians'. *Proceedings. Biological sciences* 282 (1821), 20152210.

Brazeau, M. D. & Friedman, M. 2015: The origin and early phylogenetic history of jawed vertebrates. *Nature* 520 (7548), 490–497.

Burrow, C. J.; Blaauwen, J. den; Newman, M. 2020: A redescription of the three longest-known species of the acanthodian *Cheiracanthus* from the Middle Devonian of Scotland. *Palaeontologia Electronica* 23(1): a15.

Burrow, C. J.; Davidson, R. G.; Den Blaauwen, J. L.; Newman, M. J. 2015: Revision of *Climatius reticulatus* Agassiz, 1844 (Acanthodii, Climatiidae), from the Lower Devonian of Scotland, based on new histological and morphological data. *Journal of Vertebrate Paleontology* 35 (3), e913421.

Burrow, C. J.; Newman, M.; Blaauwen, J. den; Jones R.; Davidson, R. G. 2018: The Early Devonian ischnacanthiform acanthodian *Ischnacanthus gracilis* (Egerton, 1861) from the Midland Valley of Scotland. *Acta geologica Polonica* 68 (3), 335–362.

Burrow, C. J. & Rudkin, D. 2014: Oldest Near-Complete Acanthodian: The First Vertebrate from the Silurian Bertie Formation Konservat-Lagerstätte, Ontario. *Plos One* 9 (8), e104171.

Burrow, C. J.; Trinajstic, K.; Long, J. 2012: First acanthodian from the Upper Devonian (Frasnian) Gogo Formation, Western Australia. *Historical Biology* 24 (4), 349–357.

Cabrera, D. Alfredo; C., Alberto L.; Cozzuol, M. A. 2012: Tridimensional Angel Shark Jaw elements (Elasmobranchii, Squatinidae) from the Miocene of Southern Argentina. *Ameghiniana* 49 (1), 126–131.

Caplan, M. L.& Bustin, R. M. 1999: Devonian–Carboniferous Hangenberg mass extinction event, widespread organic-rich mudrock and anoxia: causes and consequences. *Palaeogeography, Palaeoclimatology, Palaeoecology* 148 (4) 187-207.

Chen, D., Tucker, M., Shen, Y., Yans, J., Preat, A., 2002. Carbon isotope excursions and sea-level change: implications for the Frasnian–Famennian biotic crisis. J. Geol. Soc. 159, 623–626.

Chen, D., Wang, J., Racki, G., Li, H., Wang, C., Ma, X., Whalen, M.T., 2013. Large sulphur isotopic perturbations and oceanic changes during the Frasnian–Famennian transition of the Late Devonian. J. Geol. Soc. 170, 465–476.

Coates, M. I.; Finarelli, J. A.; Sansom, I. J.; Andreev, P. S.; Criswell, K. E.; Tietjen, K.; Rivers, M. L.; La Riviere, P. J. 2018: An early chondrichthyan and the evolutionary assembly of a shark body plan. *Proceedings. Biological sciences* 285, 20172418, 10 pp. http://dx.doi.org/10.1098/rspb.2017.2418

Coates, M. I.; Gess, R. W. 2007: A new reconstruction of *Onychoselache traquairi*, comments on early chondrichthyan pectoral girdles and hybodontiform phylogeny. *Palaeontology* 50 (6), 1421–1446.

Coates, M. I.; Gess, R. W.; Finarelli, J. A.; Criswell, K. E.; Tietjen, K. 2017: A symmoriiform chondrichthyan braincase and the origin of chimaeroid fishes. *Nature* 541 (7636), 208–211.

Coates, M. I.; Sequeira, S. E. K. 2001: A new stethacanthid chondrichthyan from the lower Carboniferous of Bearsden, Scotland. In *Journal of Vertebrate Paleontology* 21 (3), 438–459.

Coates, M. I.; Tietjen, Kristen; O, Aaron M.; Finarelli, J. A. 2019: High-performance suction feeding in an early elasmobranch. In *Science advances* 5 (9), eaax2742.

Davis, S. P.; Finarelli, J. A.; Coates, M. I. 2012: *Acanthodes* and shark-like conditions in the last common ancestor of modern gnathostomes. *Nature* 486 (7402), 247–250.

Deakin, W. J., Anderson, P. S. L., den Boer, W., Smith, T. J., Hill, J., Rücklin, M., Donoghue, P. C. J., Rayfield, E. J. 2022: Increasing morphological disparity and decreasing optimality for jaw speed and strength during the radiation of jawed vertebrates. *Science Advances* 8, eabl3644

Dean M.N. & Summers A.P. 2006. Mineralized cartilage in the skeleton of chondrichthyan fishes. *Zoology* 109, 164–168.

Dearden, R. P.; Giles, S. 2021: Diverse stem-chondrichthyan oral structures and evidence for an independently acquired acanthodid dentition. *Royal Society open science* 8 (11), 210822.

DeLaurier, A. & Gerhart, J. 2018: Evolution and development of the fish jaw skeleton. *Wiley Interdisciplinary Reviews*: *Developmental Biology* 8. 10.1002/wdev.337.

den Blaauwen, J.; Newman, M.; Burrow, C. 2019: A new cheiracanthid acanthodian from the Middle Devonian (Givetian) Orcadian Basin of Scotland and its biostratigraphic and biogeographical significance. *Scottish Journal of Geology* 55, 166-177.

Deng, F.; Liu, X.; Yu, H.; Yoa, Y.; Zhang, Z.; Wei, W.; Li, R. 2021: Devonian-Carboniferous Hangenberg Crisis in South China: Variations in Trace Elements, Strontium and Carbon Isotope Chemostratigraphy in Nanbiancun Carbonate Section. *Acta Geologica Sinica - English Edition,* (IF1.886).

Derycke, C.; Olive, S.; Groessens, E.; Goujet, D. 2015: Paleogeographical and paleoecological constraints on paleozoic vertebrates (chondrichthyans and placoderms) in the Ardenne Massif Shark radiations in the Famennian on both sides of the Palaeotethys. *Palaeogeography, Palaeoclimatology, Palaeoecology* 414, 61–67

Derycke, C.; Spalletta, C.; Perri, M. C., Corradini 2008: Famennian chondrichthyan microremains from Morocco and Sardinia. *Journal of Palaeontology* 82 (5), 984–995.

Destombes, J. & Hollard, H. 1988: Todrha – Ma'der, echelle 1:200,000. In Fetah, S.E.M., Bensaïd, M.M., & Dahmani., M.M. (eds): Carte Géologique du Maroc. *Notes et Mémoires du Service Géologique du Maroc. Rabat.*

Dick, J. R. F. 1981: *Diplodoselache woodi* gen. et sp. nov., an early Carboniferous shark from the Midland Valley of Scotland. *Earth and Environmental Science Transactions of The Royal Society of Edinburgh* 72 (2), 99–113.

Du, Y., Gong, Y., Zeng, X., Huang, H., Yang, J., Zhang, Z., Huang, Z., 2008. Devonian Frasnian–Famennian transitional event deposits of Guangxi, South China and their possible tsunami origin. Sci. China Ser. D Earth Sci. 51, 1570–1580.

Fields, B.D., Melott, A.L., Ellis, J., Ertel, A.F., Fry, B.J., Lieberman, B.S., Liu, Z., Miller, J.A., Thomas, B.C. 2020. Supernova triggers for end-Devonian extinctions. *PNAS* 117, 21008–21010. doi:10.1073/pnas.2013774117

Finarelli, J. A. & Coates, M. I. 2014: *Chondrenchelys problematica* (Traquair, 1888) redescribed: a Lower Carboniferous, eel-like holocephalan from Scotland. *Earth and Environmental Science Transactions of The Royal Society of Edinburgh* 105 (1), 35–59.

Frey, L., Coates, M. I., Ginter, M., Hairapetian, V., Rücklin, M., Jerjen, I., Klug, C. 2019: The early elasmobranch *Phoebodus*: phylogenetic relationships, ecomorphology, and a new time-scale for shark evolution. *Proceedings of the Royal Society B*, 20191336, 1-11.

Frey, L.; Coates, M. I.; Tietjen, K.; Rücklin, M.; Klug, C. 2020: A symmoriiform from the Late Devonian of Morocco demonstrates a derived jaw function in ancient chondrichthyans. *Communications Biology* 3 (1), 681, 1-10.

Frey, L.; Rücklin, M.; Korn, D.; Klug, C. 2018: Late Devonian and Early Carboniferous alpha diversity, ecospace occupation, vertebrate assemblages and bio-events of southeastern Morocco. *Palaeogeography Palaeoclimatology Palaeoecology* 496, 1–17.

Galili, T.; Benjamini, Y.; Simpson, G.; Jefferis, G.; Gallotta, M.; Renaudie, J.; Hennig, C. 2019: Dendextend: Extending'dendrogram'functionality in R. *R package version* 1.12. 0.

Giles, S.; Friedman, M.; Brazeau, M. D. 2015: Osteichthyan-like cranial conditions in an Early Devonian stem gnathostome. *Nature* 520 (7545), 82–85.

Ginter, M.; Hairapetian, V.; Klug, C. 2002: Famennian chondrichthyans from the shelves of North Gondwana. *Acta geologica Polonica* 52 (2), 169–215.

Ginter, M. & Maisey, J. G. (2007): The braincase and jaws of *Cladodus* from the Lower Carboniferous of Scotland. In *Palaeontology* 50 (2), 305–322. DOI: 10.1111/j.1475-4983.2006.00633.x.

Hanke, G. F.; Davis, S. P.; Wilson, M. V. H. 2001: New Species of the Acanthodian Genus Tetanopsyrus from Northern Canada, and Comments on Related Taxa. *Journal of Vertebrate Paleontology* 21 (4), 740–753.

Hanke, G. F.; Wilson, M. V. H. 2006: Anatomy of the early Devonian acanthodian *Brochoadmones milesi* based on nearly complete body fossils, with comments on the evolution and development of paired fins. *Journal of Vertebrate Paleontology* 26 (3), 526–537.

Harris, J. E. 1938: The neurocranium and jaws of *Cladoselache*. *Scientific publications of the cleveland museum of natural history* 1, 1-12.

Herbert, A. M. & Motta, P. J. 2018: Biomechanics of the jaw of the durophagous bonnethead shark. *Zoology* 129, 54-58.

Hill, J. J.; Puttick, M. N.; Stubbs, T. L.; Rayfield, E. J.; D., Philip C. J. 2018: Evolution of jaw disparity in fishes. *Palaeontology* 61 (6), 847–854.

Hodnett, J. P. M.; Grogan, E.; Lund, R.; Lucas, S. G.; Elliott, D. 2021: Ctenacanthiform sharks from the Late Pennsylvanian (Missourian) Tinajas member of the Atrasado formation, central New Mexico: *New Mexico Museum of Natural History and Science Bulletin* 84, 391-424.

Johanson, Zerina; Underwood, Charlie; Richter, Martha (Eds.)- 2018: Evolution and Development of Fishes. *Cambridge University Press*.

Kaiser, S. I.; Aretz, M.; Becker, R. T. 2015: The global Hangenberg Crisis (Devonian–Carboniferous transition): review of a first-order mass extinction. *Geological Society, London, Special Publications* 423 (1), 387–437.

Kaiser, S. I.; Becker, R. T.; Steuber, T.; Aboussalam, S. Z. 2011: Climate-controlled mass extinctions, facies, and sea-level changes around the Devonian–Carboniferous boundary in the eastern Anti-Atlas (SE Morocco). *Palaeogeography Palaeoclimatology Palaeoecology* 310 (3-4), 340–364.

Kemp, N. E. &Westrin, S. K. 1979: Ultrastructure of calcified cartilage in the endoskeletal tesserae of sharks. *Journal of morphology* 160 (1), 75–109.

Klug, C.; Frey, L.; Korn, D.; Jattiot, R.; Rücklin, M. 2016: The oldest Gondwanan cephalopod mandibles (Hangenberg Black Shale, Late Devonian) and the mid-Palaeozoic rise of jaws. *Palaeontology* 59 (5), 611–629.

Klug, C.; Lagnaoui, A.; Jobbins, M.; Bel Haouz, W.; Najih., A. 2021: The swimming trace *Undichna* from the latest Devonian Hangenberg Sandstone equivalent of Morocco. *Swiss Journal of Palaeontology* 140 (1), 19.

Klug, S. & Kriwet, J. 2008: A new basal galeomorph shark (Synechodontiformes, Neoselachii) from the Early Jurassic of Europe. *Naturwissenschaften* 95 (5), 443–448.

Lane, J. A.& Maisey, J. G. 2012: The visceral skeleton and jaw suspension in the durophagous hybodontid shark *Tribodus limae* from the Lower Cretaceous of Brazil. *Journal of Palaeontology* 86 (5), 886–905.

Letsch, D.; Large, S. J.E.; Bernasconi, S.; Klug, C.; Blattmann, T.; Winkler, W.; von Quadt, A. 2018: Northwest Africa's Ediacaran to early Cambrian fossil record, its oldest metazoans and age constraints for the basal Taroudant Group (Morocco). *Elsevier Oceanography Series* 320, 438-453.

Long, J. A.; Burrow, C. J.; Ginter, M.; Maisey, J. G.; Trinajstic, K. M.; Coates, M. I.; Young, G. C.; Senden, T. J. 2015: First shark from the Late Devonian (Frasnian) Gogo Formation, Western Australia sheds new light on the development of tessellated calcified cartilage. *Plos one* 10 (5), e0126066.

Luccisano, V.; Pradel, A.; Amiot, R.; Gand, G.; Steyer, J. S.; Cuny, G. 2021: A new *Triodus* shark species (Xenacanthidae, Xenacanthiformes) from the lowermost Permian of France and

its paleobiogeographic implications. *Journal of vertebrate Palaeontology* 41 (2), 1-18. DOI: 10.1080/02724634.2021.1926470

Maisey, J. G. 1985: Cranial morphology of the fossil elasmobranch *Synechodus dubrisiensis. American Museum novitates* no. 2804: New York, N.Y.: American Museum of Natural History.

Maisey, J. G. 2013: The diversity of tessellated calcification in modern and extinct chondrichthyans. *Revue de Paléobiologie* 32 (2), 355–371.

Maisey, J. G.; Denton, J. S. S.; Burrow, C.; Pradel, A. 2020: Architectural and ultrastructural features of tessellated calcified cartilage in modern and extinct chondrichthyan fishes. *Journal of fish biology* 98 (4), 919–941.

Maisey, J. G.; Janvier, P.; Pradel, A.; Denton, J. S. S.; Bronson, A.; Miller, R.; Burrow, C. J. 2018: *Doliodus* and pucapampellids: Contrasting perspectives on stem chondrichthyan morphology. In Johanson, Z., Underwood, C., Richter, M. (Eds.): Evolution and Development of Fishes. *Cambridge University Press*, 87–109.

McGhee, G.R., 1996: The Late Devonian Mass Extinction: The Frasnian/Famennian Crisis. *Columbia Universtiy Press, New York.*

McGhee, G.R., Sheehan, P.M., Bottjer, D.J., Droser, M.L., 2012: Ecological ranking of Phanerozoic biodiversity crises: the Serpukhovian (Early Carboniferous) crisis had a greater ecological impact than the end-Ordovician. *Geology* 40, 147–150.

McGhee, G. R., Clapham, M. E., Sheehan, P. M., Bottjer, D. J., Droser, M. L., 2013. A new ecological-severity ranking of major Phanerozoic biodiversity crises. *Palaeogeography, Palaeoclimatology, Palaeoecology* 370, 260–270.

Morrow, J. R., Sandberg, C. A. 2005: Revised dating of Alamo and some other Late Devonian impacts in relation to resulting mass extinction. *68th Annual Meteoritical Society Meeting*, 1 p.

Motta, P. J., Huber, D. R. 2012: Prey capture behavior and feeding mechanics of elasmobranchs. In: Carrier, J. C., Musick, J. A., Heithaus, M. R. (Eds.), Biology of Sharks and Their Relatives. *CRC Press, Boca Raton, FL* pp. 153–209.

Paschall, O.; Carmichael, S. K.; Königshof, P.; Waters, J. A.; Ta, P. H.; Komatsu, T.; Dombrowski, A. 2019: The Devonian-Carboniferous boundary in Vietnam: Sustained ocean anoxia with a volcanic trigger for the Hangenberg Crisis? *Global and Planetary Change* 175, 64-81.

Pisarzowska A.; Raconciński M.; Marynowsky L.; Szczerba, M.; Thoby, M.; Paszkowski, M.; Perri, M. C.; Spaletta, C.; Schönlaub, H. P.; Kowalik, N.; Gereke, M. 2020: Large environmental disturbances caused by magmatic activity during the Late Devonian Hangenberg Crisis. *Global and Planetary Change* 190, 103155.

Pradel, A.; Maisey, J. G.; Tafforeau, P.; Mapes, R. H.; Mallatt, J. 2014: A Palaeozoic shark with osteichthyan-like branchial arches. *Nature* 509 (7502), 608–611.

Qiao, T.; King, B.; Long, J. A.; Ahlberg, P. E.; Zhu, M. 2016: Early Gnathostome Phylogeny Revisited: Multiple Method Consensus. *Plos one* 11 (9), e0163157.

R Development Core Team. 2020: R: A Language and Environment for Statistical Computing. *R Foundation for Statistical Computing,* Vienna, Austria, pp.

Racki, G., Marynowski, L. & Rakociński, M. 2018. Anomalous Upper Devonian mercury enrichments: comparison of inductively coupled plasma – mass spectrometry (ICP-MS) and atomic absorption spectrometry (AAS) analytical data. *Geological Quarterly* 62, 487–495.

Rakociński, M., Marynowski, L., Pisarzowska, A., Bełdowski, J., Siedlewicz, G., Zatoń, M., Perri, M. C., Spalletta, C. & Schönlaub, H. P. 2020. Volcanic related methylmercury poisoning as the possible driver of the end-Devonian Mass extinction. *Scientific Reports* 10:7344, 1-4.

Rieppel, O. 1981: The hybodontiform sharks from the Middle Triassic of Monte San Giorgio, Switzerland. *Neues Jahrbuch für Geologie und Paläontologie* 161 (3), 324 - 353.

Rohlf, F. J. 2015: The tps series of software. *Hystrix, the Italian Journal of Mammalogy* 26:9–12.

Romano, C. & Brinkmann, W. 2010: A new specimen of the hybodont shark *Palaeobates polaris* with three-dimensionally preserved Meckel's cartilage from the Smithian (Early Triassic) of Spitsbergen. *Journal of Vertebrate Paleontology* 30 (6), 1673–1683.

Rücklin, M.; King, B.; Cunningham, J. A.; Johanson, Z.; Marone, F.; Donoghue, P. C. J. 2021: Acanthodian dental development and the origin of gnathostome dentitions. *Nature Ecology and Evolution* 5 (7), 919–926.

Sallan, L. C. & Coates, M. I. 2010: End-Devonian extinction and a bottleneck in the early evolution of modern jawed vertebrates. *Proceedings of the National Academy of Sciences of the United States of America* 107 (22), 10131–10135.

Sandberg, C.A., Ziegler, W., Dreesen, R., Butler, J.L., 1988. Late Frasnian mass extinction: conodont event stratigraphy, global changes, and possible causes. *Courier Forschungstinstitut Senckenberg* 102, 263–307.

Schultze, H. P.; Zidek, N. J. 1982: Ein primitiver acanthodier (pisces) aus dem Unterdevon Lettlands. *Paläontologische Zeitschrift* 56 (1-2), 95–105.

Seidel R, Blumer M, Chaumel J, Amini S, Dean M.N. 2020. Endoskeletal mineralization in chimaera and a comparative guide to tessellated cartilage in chondrichthyan fishes (sharks, rays and chimaera). *Journal of the Royal Society Interface*. 17 (171), 20200474.

Seidel, R.; Jayasankar, A. K.; Dean, M. N. 2021: The multiscale architecture of tessellated cartilage and its relation to function. *Journal of fish biology* 98 (4), 942–955.

Seidel, R.; Lyons, K.; Blumer, M.; Zaslansky, P.; Fratzl, P.; Weaver, J. C.; Dean, M. N. 2016: Ultrastructural and developmental features of the tessellated endoskeleton of elasmobranchs (sharks and rays). *Journal of anatomy* 229 (5), 681–702.

Tribovillard, N., Averbuch, O., Devleeschouwer, X., Racki, G., Riboulleau, A., 2004. Deep-water anoxia over the Frasnian–Famennian boundary (La Serre, France): a tectonically induced oceanic anoxic event? *Terra Nova* 16, 288–295.

Wilga; C. D. & Motta, P. J. 1998: Conservation and variation in the feeding mechanism of the spiny dogfish squalus acanthias. *The Journal of experimental biology* 201 (9), 1345–1358.

Zangerl, R.; Case, G. R. 1976: Cobelodus aculeatus (Cope) an anacanthous shark from Pennsylvanian Black Shales of North America. *Palaeontographica, Sonder Abdruck* 154, 107–157.

Zhu, M.; Yu, X.; Ahlberg, P. E.; Choo, B.; Lu, J.; Qiao, T. et al. 2013: A Silurian placoderm with osteichthyan-like marginal jaw bones. *Nature* 502 (7470), 188–193.

Figure 1

Meckel's cartilage outlines and close ups

Meckel's cartilage of an ischnacanthiform acanthodian from the Hangenberg black shale, Madene El Mrakib; PIMUZ A/I 5139. A, medial view; B_1, traced outline; B_2, counterpart with outline; $C_{1,2}$, Close-up photos of the cartilage showing the polygonal pattern. Abbreviations: sym - symphysis, ma - muscle attachment area, vr - ventral ridge, re.fl - retroarticular flange.

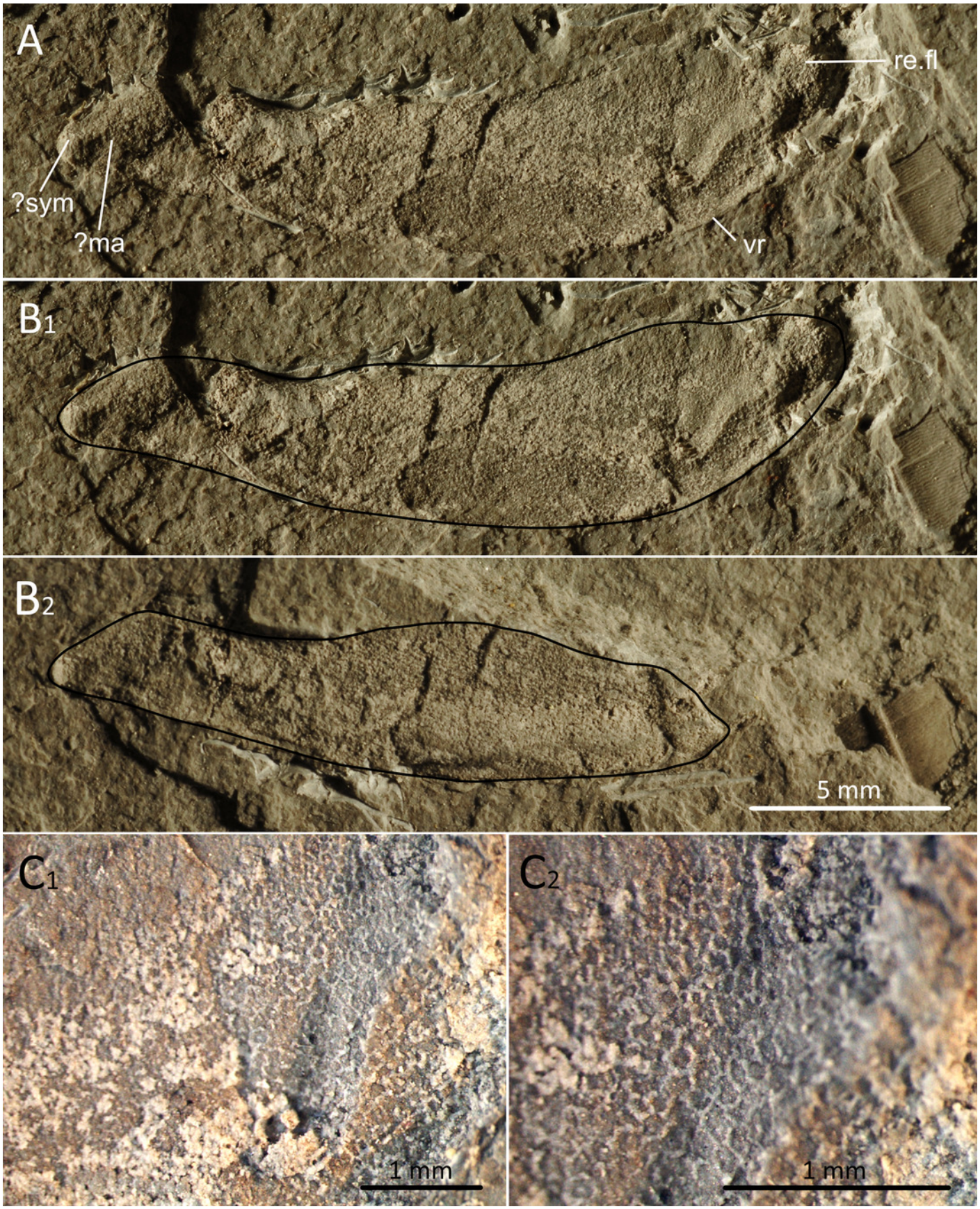
A
re.fl
?sym
?ma
vr
B1
B2
5 mm
C1
1 mm
C2
1 mm

Figure 2

PCA and morphospace with all sampled lower jaws

Principal Component Analysis of some fossil and modern chondrichthyan lower jaws. Orange colours: acanthodians; purple colours: holocephalan; blue colours: elasmobranchs. The new lower jaw from the Hangenberg black shale is represented by a black dot and grey colours represent lower jaws of unknown class and order. A jaw morphospace is represented in the background showing the shape variation. The new Hangenberg black shale jaw plots close to jaws of acanthodians as well as elasmobranchs. Lv: Latviacanthus ventspilsensis, Is: Ischnacanthus sp., Po: Palidiplospinax occultidens, Dh: Dracopristis hoffmanorum, Ct: Ctenacanthus sp. Hd: Heslerodus divergens

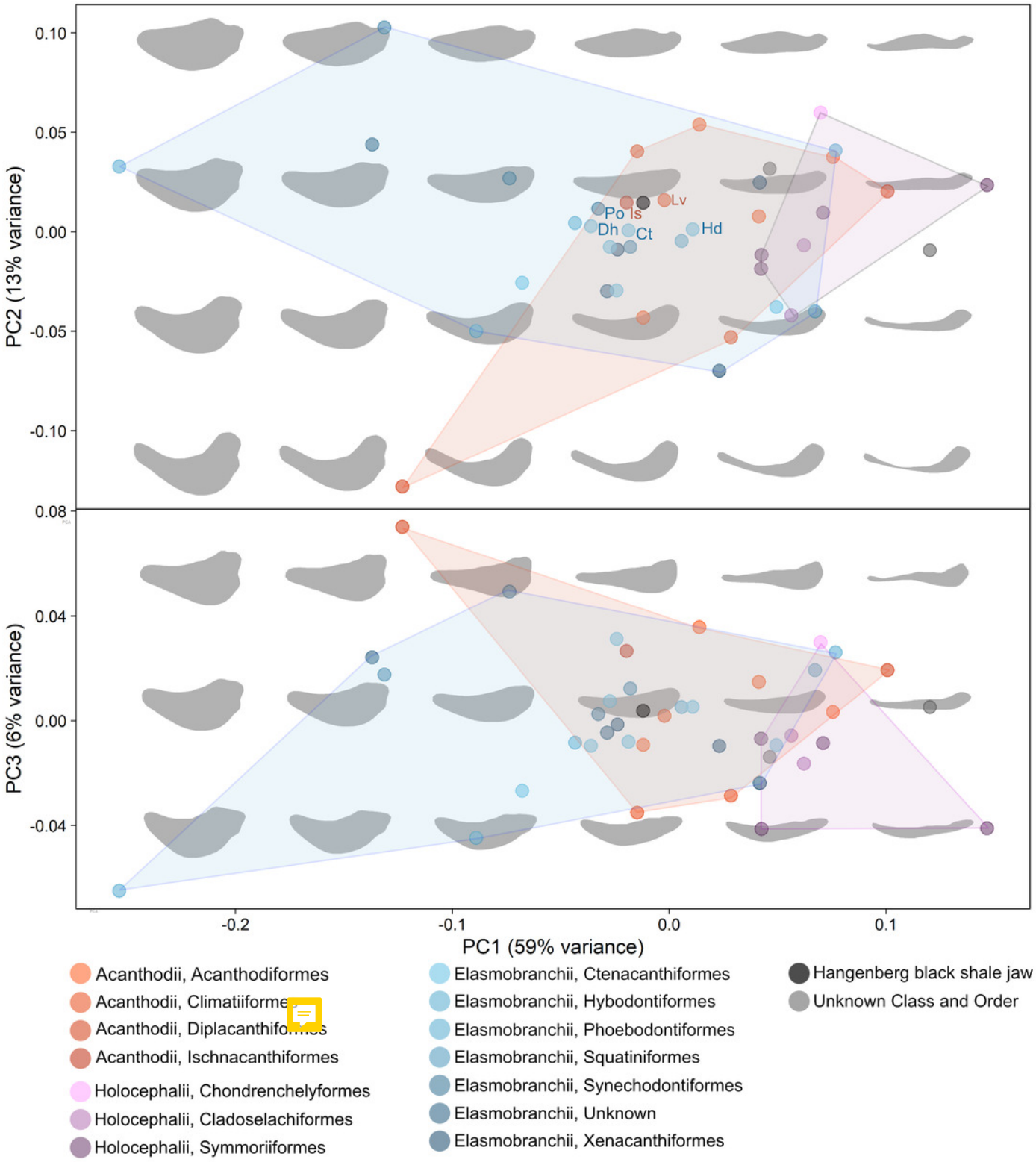
PC2 (13% variance)
PC3 (6% variance)
PC1 (59% variance)
0.10
0.05
0.00
-0.05
-0.10
0.08
0.04
0.00
-0.04
-0.2
-0.1
0.0
0.1
Po
Is
Lv
Dh
Ct
Hd
Acanthodii, Acanthodiformes
Acanthodii, Climatiiformes
Acanthodii, Diplacanthiformes
Acanthodii, Ischnacanthiformes
Holocephalii, Chondrenchelyformes
Holocephalii, Cladoselachiformes
Holocephalii, Symmoriiformes
Elasmobranchii, Ctenacanthiformes
Elasmobranchii, Hybodontiformes
Elasmobranchii, Phoebodontiformes
Elasmobranchii, Squatiniformes
Elasmobranchii, Synechodontiformes
Elasmobranchii, Unknown
Elasmobranchii, Xenacanthiformes
Hangenberg black shale jaw
Unknown Class and Order

Figure 3

Dendrogram showing morphological distances of the sampled lower jaws

Dendrogram showing morphological distances regarding the first principal components from the PCA. Orange colours: acanthodians; purple colours: holocephalan; blue colours: elasmobranchs. The elasmobranchs plot mainly on the top, while holocephalan jaws plot mainly at the bottom. Acanthodian jaws are scattered over the whole dendrogram. The lower jaw from the Hangenberg black shale is closest to some acanthodian jaws such as that of Ischnacanthus sp.

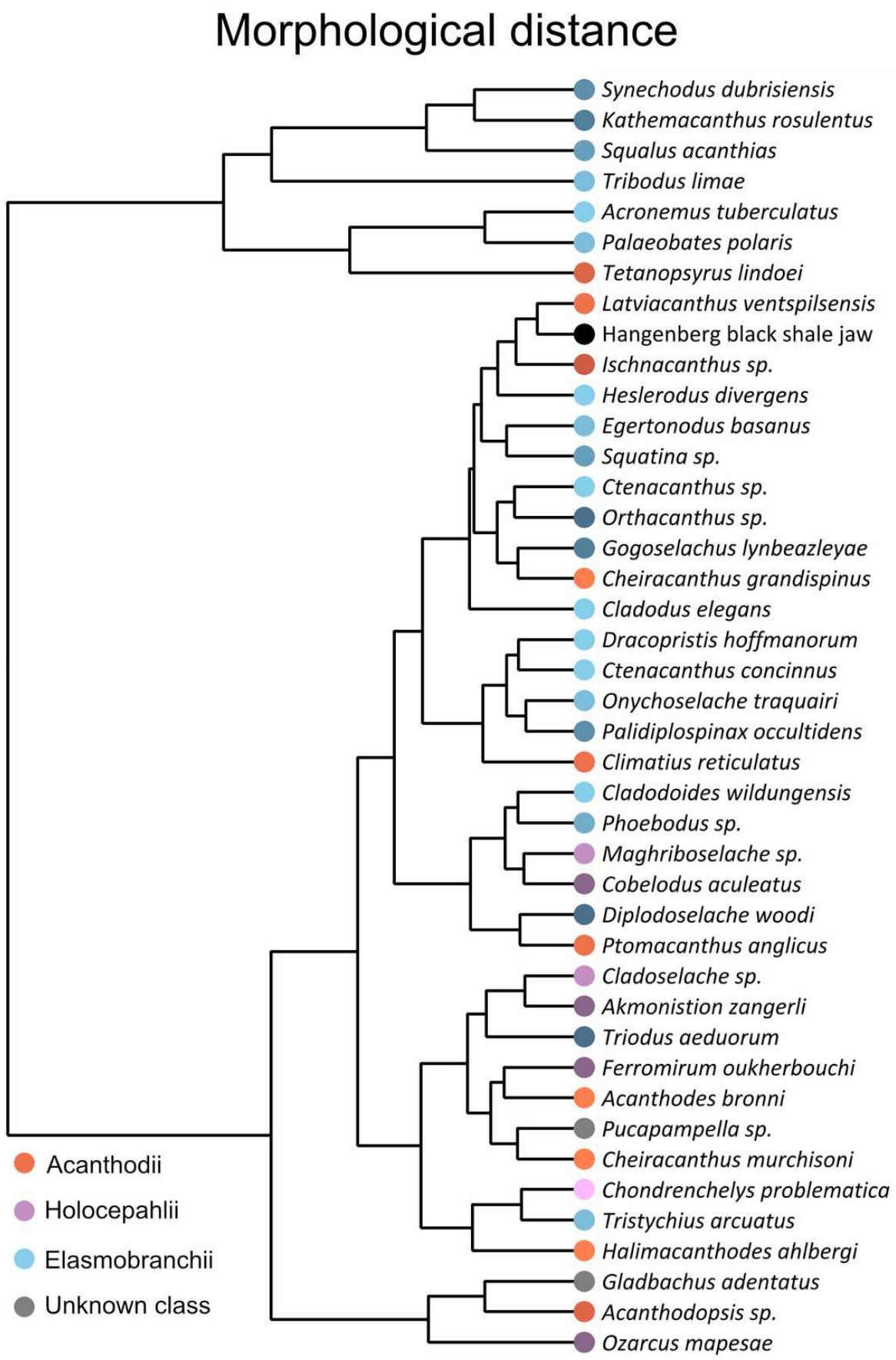
Morphological distance
Synechodus dubrisiensis
Kathemacanthus rosulentus
Squalus acanthias
Tribodus limae
Acronemus tuberculatus
Palaeobates polaris
Tetanopsyrus lindoei
Latviacanthus ventspilsensis
Hangenberg black shale jaw
Ischnacanthus sp.
Heslerodus divergens
Egertonodus basanus
Squatina sp.
Ctenacanthus sp.
Orthacanthus sp.
Gogoselachus lynbeazleyae
Cheiracanthus grandispinus
Cladodus elegans
Dracopristis hoffmanorum
Ctenacanthus concinnus
Onychoselache traquairi
Palidiplospinax occultidens
Climatius reticulatus
Cladodoides wildungensis
Phoebodus sp.
Maghriboselache sp.
Cobelodus aculeatus
Diplodoselache woodi
Ptomacanthus anglicus
Cladoselache sp.
Akmonistion zangerli
Triodus aeduorum
Ferromirum oukherbouchi
Acanthodes bronni
Pucapampella sp.
Cheiracanthus murchisoni
Chondrenchelys problematica
Tristychius arcuatus
Halimacanthodes ahlbergi
Gladbachus adentatus
Acanthodopsis sp.
Ozarcus mapesae
Acanthodii
Holocepahlii
Elasmobranchii
Unknown class

Figure 4

Mantel test results

Results of the Mantel test analysis performed in 1000 trees accounting for phylogenetic and stratigraphic uncertainty. R statistic values close to 1 or -1 support strong correlation, while values close to 0 support weak correlation

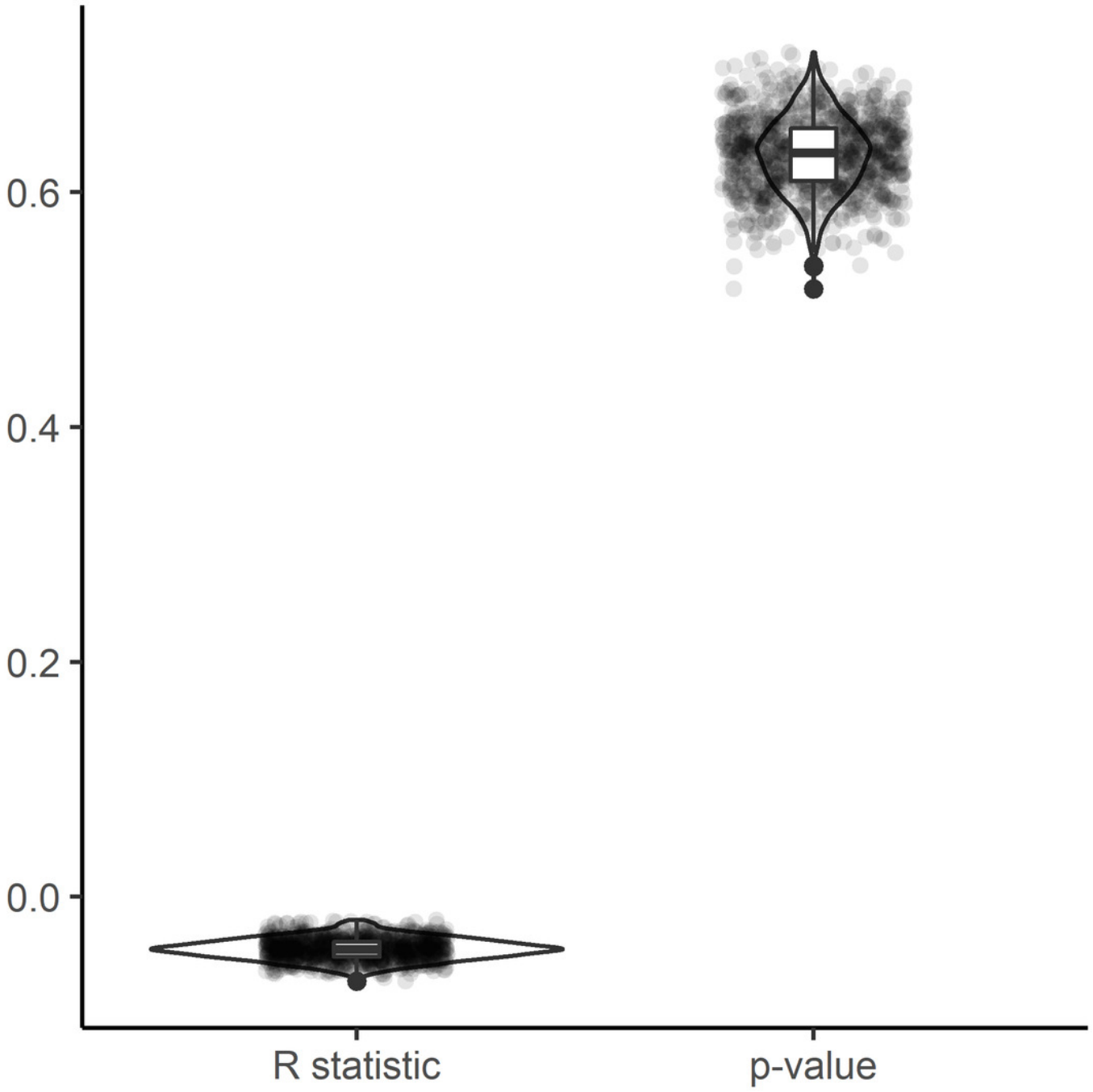
0.6
0.4
0.2
0.0
R statistic
p-value

Figure 5

visual jaw shape comparison

Visual comparison of the new HBS Meckel's cartilage (grey, top) with the two most similar jaw shapes of two different groups (pink, middle) and an overlay of both (pink and grey, bottom). A: the elasmobranch Heslerodus divergens. B: the acanthodian Ischnacanthus sp. Different characteristic points are correlated and both shapes are shown in overlap with the HBS Meckel's cartilage.

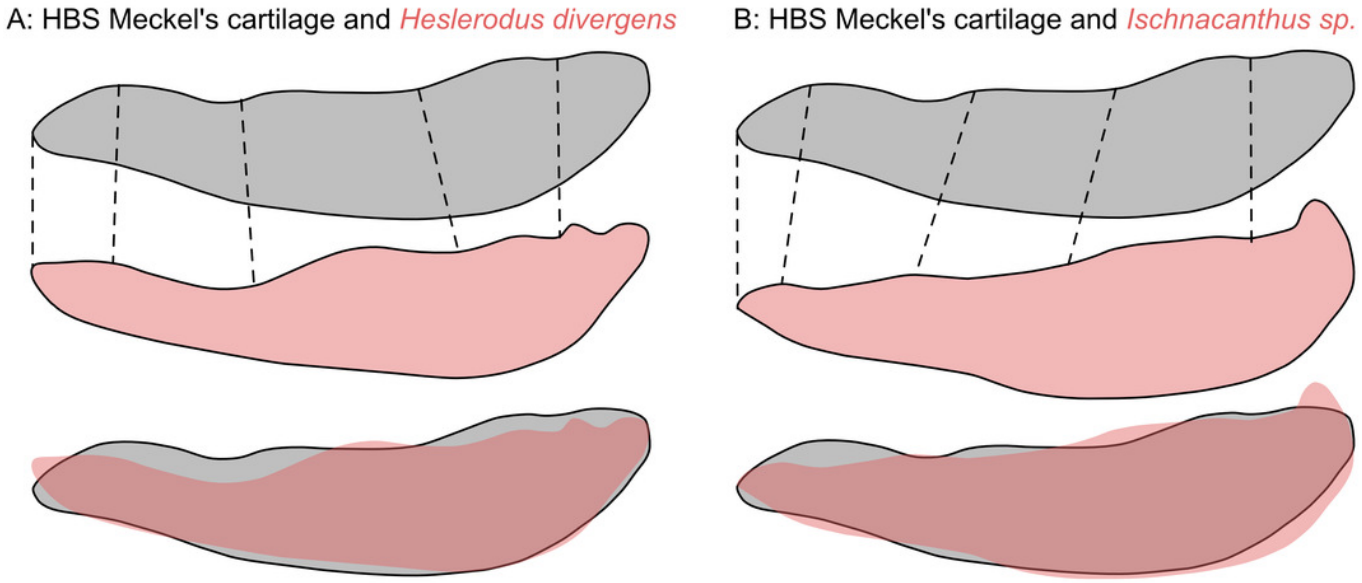

Figure 6

All sampled outlines in a phylogenetic tree showing the possible position of the new Meckel's cartilage

Simplified chondrichthyan phylogeny modified after Klug et al. (in prep.). The lower jaw from the Hangenberg black shale is figured together with the taxa used in the Fourier Analysis. The shapes of the lower jaws were redrawn from the literature (App. 1). The new HBS jaw is suggested to be of ctenacanthiform origin. Another possible origin is an ischnacanthiform

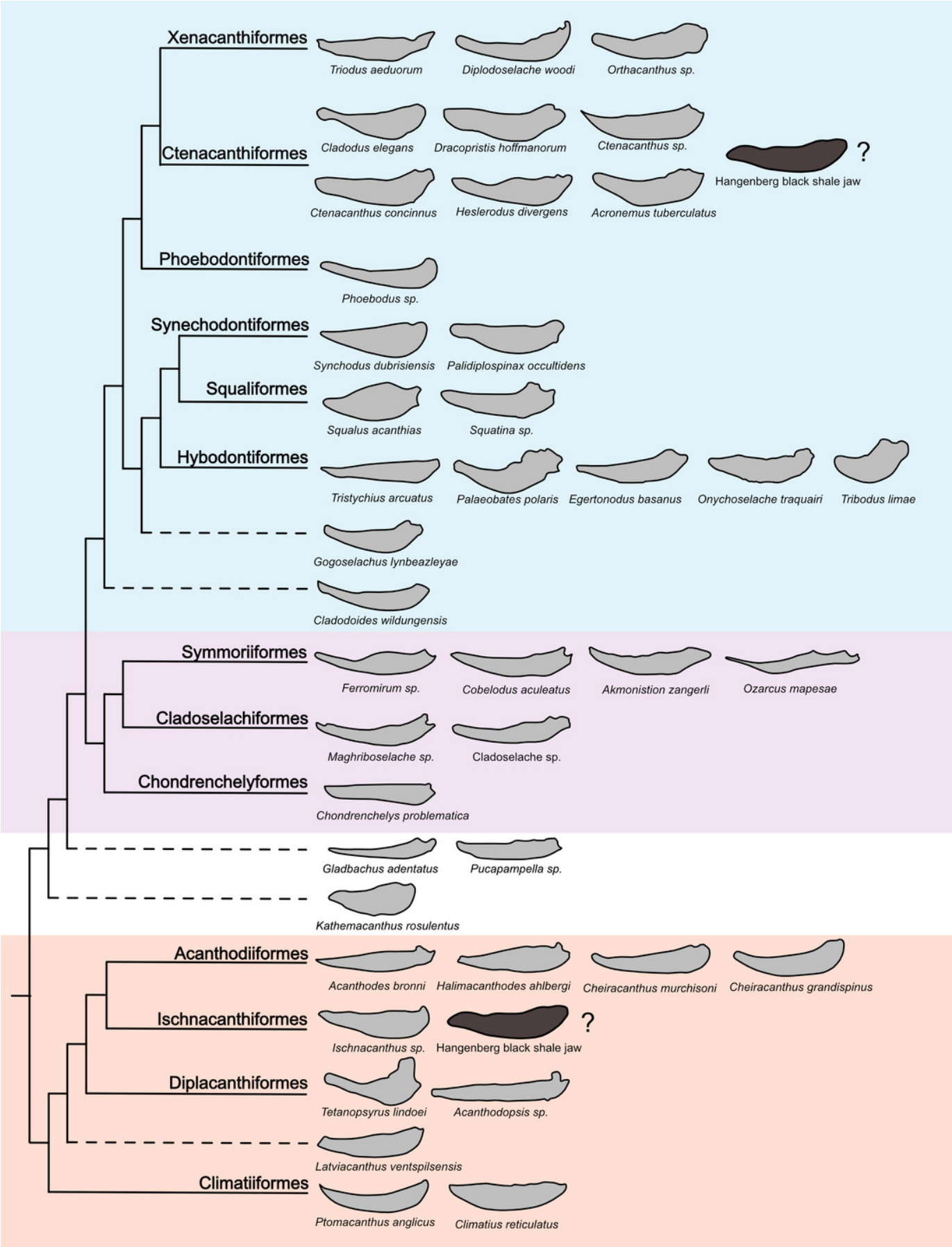
Xenacanthiformes
Triodus aeduorum
Diplodoselache woodi
Orthacanthus sp.
Ctenacanthiformes
Cladodus elegans
Dracopristis hoffmanorum
Ctenacanthus sp.
?
Hangenberg black shale jaw
Ctenacanthus concinnus
Heslerodus divergens
Acronemus tuberculatus
Phoebodontiformes
Phoebodus sp.
Synechodontiformes
Synchodus dubrisiensis
Palidiplospinax occultidens
Squaliformes
Squalus acanthias
Squatina sp.
Hybodontiformes
Tristychius arcuatus
Palaeobates polaris
Egertonodus basanus
Onychoselache traquairi
Tribodus limae
Gogoselachus lynbeazleyae
Cladodoides wildungensis
Symmoriiformes
Ferromirum sp.
Cobelodus aculeatus
Akmonistion zangerli
Ozarcus mapesae
Cladoselachiformes
Maghriboselache sp.
Cladoselache sp.
Chondrenchelyformes
Chondrenchelys problematica
Gladbachus adentatus
Pucapampella sp.
Kathemacanthus rosulentus
Acanthodiiformes
Acanthodes bronni
Halimacanthodes ahlbergi
Cheiracanthus murchisoni
Cheiracanthus grandispinus
Ischnacanthiformes
Ischnacanthus sp.
?
Hangenberg black shale jaw
Diplacanthiformes
Tetanopsyrus lindoei
Acanthodopsis sp.
Latviacanthus ventspilsensis
Climatiiformes
Ptomacanthus anglicus
Climatius reticulatus